Orientational Motions of Vibrational Chromophores in Molecules at the Air/Water Interface with Time-Resolved Sum Frequency Generation

Yi Rao, Daohua Song, Nicholas J. Turro, and Kenneth B. Eisenthal*

Department of Chemistry, 3000 Broadway, Columbia University, New York, New York 10027

Received: March 21, 2008; Revised Manuscript Received: July 11, 2008

The first time-resolved experiments in which interfacial molecules are pumped to excited electronic states and probed by vibrational sum frequency generation (SFG) are reported. This method was used to measure the out-of-plane rotation dynamics, i.e. time dependent changes in the polar angle, of a vibrational chromophore of an interfacial molecule. The chromophore is the carbonyl group, the rotation observed is that of the $-C=O$ bond axis, with respect to the interfacial normal, and the interfacial molecule is coumarin 314 (C314) at the air/water interface. The orientational relaxation time was found to be 220 ± 20 ps, which is much faster than the orientational relaxation time of the permanent dipole moment axis of C314 at the same interface, as obtained from pump-second harmonic probe experiments. Possible effects on the rotation of the $-C=O$ bond axis due to the carbonyl group hydrogen bonding with interfacial water are discussed. From the measured equilibrium orientation of the permanent dipole moment axis and the carbonyl axis, and knowledge of their relative orientation in the molecule, the absolute orientation of C314 at the air/water interface is obtained.

1. Introduction

The intrinsic asymmetry of an interface is responsible for its unique properties, which differ from either of the bulk media that form the interface. Thus both the static, e.g. orientational structures, chemical equilibrium, polarity, etc., and dynamic processes, e.g. orientational relaxation, intermolecular energy transfer, photoisomerization, etc., differ from the corresponding property in the bulk phase.[1−10] It is not surprising that even the apparently simple example of the air/water interface shows complex properties.[11−14,3−10] Many types of molecules dissolved in water are able to adsorb in excess to the interface to achieve a lower surface free energy. Within bulk water, these dissolved molecules can rotate and diffuse freely in all directions.[1,2] In contrast, the motions of a solute molecule at the air/water interface are restricted by the asymmetric potential at the interface. Some parts of the molecule prefer to project down into the water due to hydrophilicity, while other parts may preferentially project up into the air due to hydrophobicity. This asymmetric surface environment results in anisotropic orientational motions at a liquid interface, i.e. the dynamics of rotation in the interfacial plane differ from the out-of-plane orientational motions.[15−18]

Second harmonic generation (SHG) and sum frequency generation (SFG),[11−14,19−36] as second-order spectroscopies, are interface specific, including buried interfaces that are accessible to light. Second harmonic generation (SHG) depends primarily on the electronic properties of the interfacial molecules whereas SFG is sensitive to molecular vibrations when one of the incident beams is in the infrared. Static SHG and SFG measurements provide information about the molecular species, molecular orientational ordering, acid−base equilibrium, etc. occurring at interfaces.[12,3−10] Time-resolved SHG has been used to study solvation and rotational dynamics, electron transfer, population recovery, and other ultrafast processes.[17,37−40] Few studies using time-resolved SFG have been reported, and these studies focused on IR-pump-SFG-probe measurements[41−43]In these earlier pioneering studies of interfacial dynamics processes, an IR pulse was used to pump an interfacial chemical species to an excited vibrational state and SFG was used to probe the relaxation processes. In the studies reported here, we describe the first experiments in which interfacial molecules are pumped to excited electronic states and SFG is used to probe an ultrafast relaxation process, which in this paper is the rotational motion of a chemical group, the carbonyl $-C=O$ in the aromatic ring of C314 at the air/water interface (Figure 1). The dynamics of excited-state solvation that is probed with SFG will be reported separately. In our previous pump-SHG-probe studies of orientational relaxation, it was the rotational dynamics of a different molecular axis, namely the dipole moment axis of C314 that was measured.

2. Experimental Section

In the following, we will describe a spectral-resolved and time-resolved SFG technique. A new approach to the measurement of vibrational spectra using SFG (broadband sum frequency generation) has been developed and has proven to be successful.[30−32,44−46] It entails combining a spectrally broad IR pulse, which is characteristic of femtosecond IR pulses, with a spectrally narrow visible pulse (12 cm^{-1}). We achieve femtosecond time resolution, by using femtosecond IR light and femtosecond pump pulses. The instrument response is determined by the cross correlation time of the IR and the pump light and was 175 fs.

One 800 nm regeneratively amplified Ti:sapphire system (Spitfire, Spectra Physics) seeded with a MaiTai 80 MHz, 80 fs oscillator, at a 1 kHz repetition frequency was employed in the present experiments. The 800 nm femtosecond pulse was compressed to a 10 ps pulse with a spectral width of 12 cm^{-1} and an output energy of 8 μJ per pulse.[47] A tunable infrared light between 3 and 8.5 μm with a bandwidth of 150 cm^{-1} (fwhm) was generated using part of an 800 nm femtosecond

---

* Author to whom correspondence should be addressed. E-mail: kbe1@columbia.edu.

10.1021/jp802499w CCC: $40.75

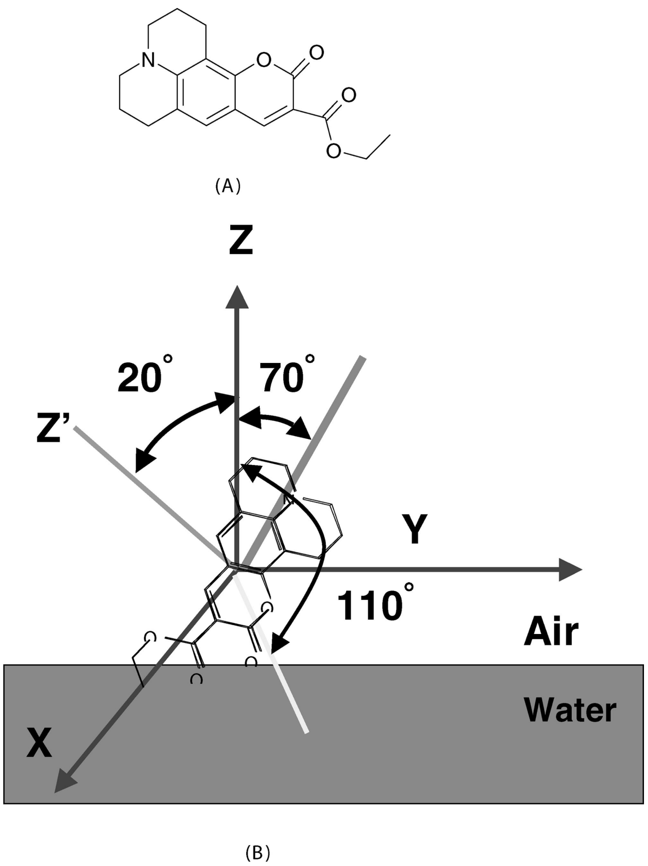

Figure 1. (A) Chemical structure of coumarin 314. (B) Absolute orientation of coumarin 314 at the air/water interface. The angle between the normal to the molecular plane and the surface normal is 20°. The electronic dipole direction with respect to the surface normal is 70°, and the carbonyl group is 110° to the surface normal.

pulse with an optical parametric amplifier (OPA) (Spectra-Physics). The remaining part of the 800 nm femtosecond pulse was used to generate a 423 nm femtosecond pump pulse with a second OPA.

The IR beam with a typical power of 1.5 μJ per pulse at 5.7 μm is focused onto the sample by a BaF_2 lens at an angle of 67° relative to the surface normal. The 400 nm picosecond light was focused at an angle of 76° to the surface normal. The 423 nm pump light was incident normal to the interface. The polarization of the circularly polarized pump beam was controlled using a quarter wave plate. A 300 mm spectrograph coupled to a charge-coupled device (CCD) camera (Acton) was used to measure the SFG spectra, and a photomultiplier tube (PMT) (Hamamatsu) was used in the time-dependent measurements.

The purity of coumarin 314 (≥99%, Aldrich) was checked by HPLC. A 16 μM solution was made using ultrapure water (resistivity 18.2 MΩ cm, Millipore Corp). The Teflon beakers were cleaned prior to use by immersion in freshly prepared piranha solution for 20 min and then rinsed with copious amounts of ultrapure water in order to remove any trace organics. The sample is contained in a shallow Teflon beaker mounted on a stage rotating at 2.5 rpm to minimize heating and degradation effects.

3. Results and Discussion

The sum frequency intensity[11] is proportional to the square of the susceptibility elements made up of a nonresonant part $\chi^{(2),NR}$ and a resonant part $\chi^{(2),R}$.

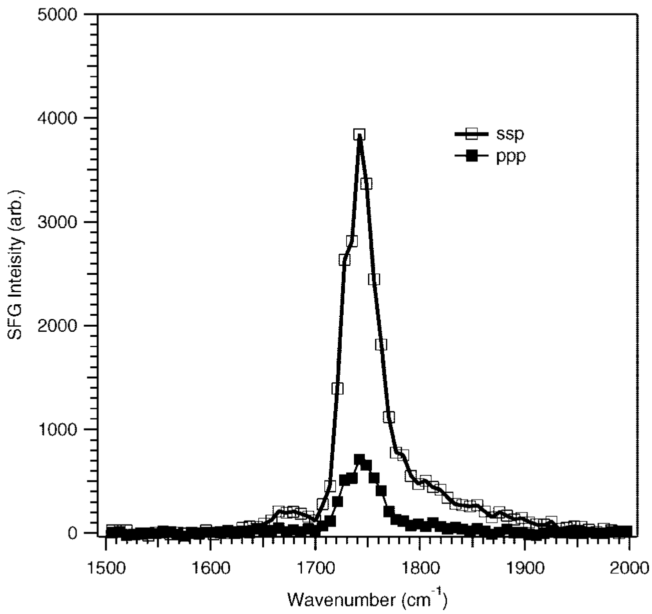

Figure 2. Sum frequency generation spectra of coumarin 314 at the air/water interface. The *SSP* and *PPP* SFG spectra are shown.

$$\begin{aligned} I^{SF}(\omega) &\propto |\chi^{(2),NR} + \sum_{q}^{n} \chi^{(2),R}(\omega,q)|^2 \\ \chi^{(2),R}(\omega,q) &\propto \frac{A_q}{\omega_{ir} - \omega_q + i\Gamma_q} \end{aligned} \tag{1}$$

where A_q contains the product of the Raman and infrared matrix elements of the qth vibration, ω_q denotes the resonant frequency of the qth vibration, ω_{ir} is the frequency of the IR light, and Γ_q is the spectral width of the vibrational state.

The two polarization combinations measured in each experiment were *SSP*, and *PPP*, where the first letter denotes the polarization of the sum frequency, the second one denotes the polarization of the 400 nm light, and the last one denotes the polarization of the IR light. These polarizations are connected with the laboratory coordinates by nonlinear Fresnel coefficients and appropriate projections.[22,48−50] Figure 2 shows that the main peak is 1738 cm^{-1} in the *SSP* polarization spectrum with a weak peak at 1680 cm^{-1}. In the *PPP* spectrum, we observed only the peak at 1738 cm^{-1}. To establish which of the two carbonyl chromophores in the coumarin 314 molecule generates the main peak, we performed an experiment on coumarin 153, whose structure is similar to the coumarin 314, but has only one carbonyl which is in the ring of the molecule. The SFG spectra of coumarin 153 only shows one peak, which is at 1725 cm^{-1}. Therefore, we assigned the main peak at 1738 cm^{-1} to the symmetric stretching mode of $-C{=}O$ in the ring of coumarin 314. The small peak at 1680 cm^{-1} is assigned to the stretching mode of the carbonyl group of the ethyl ester.

As the carbonyl group in the ring of coumarin 314 has $C_{\infty v}$ symmetry, there are three nonzero hyperpolarizability tensors, which are α^{SF}_{zzz} and $\alpha^{SF}_{xxz} = \alpha^{SF}_{yyz}$, where z is parallel to the bond axis and x and y are perpendicular. Of the total 27 macroscopic susceptibility tensors $\chi^{(2)}_{IJK}$ (I, J, and K being the three laboratory coordinates), 7 terms are nonvanishing for a rotationally isotropic interface ($C_{\infty v}$ symmetry), namely, $\chi^{(2)}_{XXZ} = \chi^{(2)}_{YYZ}$; $\chi^{(2)}_{XZX} = \chi^{(2)}_{YZY}$; $\chi^{(2)}_{ZXX} = \chi^{(2)}_{ZYY}$ and $\chi^{(2)}_{ZZZ}$. In the determination of the orientational structure of the equilibrium ground state, we used the intensity ratio method. The *YZ* plane was the plane of incidence for both the visible and IR beams. The two polarization combinations *SSP* and *PPP* can be obtained from the above nonzero macroscopic susceptibilities. The relative strengths of the SFG intensities for the *SSP* vs *PPP*, shown in Figure 2, are consistent with the relative Fresnel coefficients for the carbonyl group when oriented at polar angles greater than 50°.[14,46] To assist us in the interpretation of our results, we performed numerical calculations to obtain the relative intensities of the four polarization combinations using a specific calculation procedure.[46] Briefly, we consider the macroscopic susceptibilities and their connections with the microscopic hyperpolarizabilities under different polarization combinations. Calculations of the relative intensities of the generally used polarization combinations *SSP*, *PPP* show the relative intensities as a function of the orientational angle. The SFG intensities can be expressed into the following,

$$\begin{aligned} I^{SSP}(\omega_{\mathrm{SF}}) &\propto |\chi^{(2)}_{SSP}|^2 = |A<\cos\theta> - B<\cos^3\theta>|^2 \\ I^{PPP}(\omega_{\mathrm{SF}}) &\propto |\chi^{(2)}_{PPP}|^2 = |C<\cos\theta> - D<\cos^3\theta>|^2 \end{aligned} \qquad (2)$$

Where *A*, *B*, *C*, and *D* can be calculated from Fresnel coefficients and geometric factors.[14] We find that the orientation of the carbonyl group with respect to the interfacial normal is 70° assuming a narrow orientational distribution. Combining the SHG measurements, which yields an orientation of 70 ° for the coumarin 314 transition dipole axis, which is also the permanent dipole axis, with respect to the surface normal, we obtain the absolute orientation of the coumarin 314 molecule at the air/water interface by using the procedure described in earlier work.[46] We calculate the angle of the normal to the molecular plane with respect to the interface normal to be 20°, which is also the angle between the molecular plane and the surface plane, as shown in Figure 1.

3.1. Pump-Induced Nonequilibrium Orientational Distribution. The pump pulse photoselects an orientational subset of the equilibrium distribution of ground-state molecules, which thereby generates nonequilibrium orientational distributions in both the ground-state molecules that were not excited and the excited-state molecules produced by the pump pulse. The SFG signal is sensitive to the orientational motions that bring the ground and excited-state molecules to their equilibrium orientations. Depending on the polarization of the pump pulse, the change in the SFG intensity with time can depend on both in and out-of-plane rotations or only on out-of-plane rotations. To separate the out-of-plane rotations from in-plane rotations, a circular polarized laser pump pulse, incident normal to the interfacial plane, was used to excite C314 molecules to their lowest singlet excited state. Initially the ground-state molecules are isotropically distributed in the interfacial plane because of the inherent in-plane isotropy of the air/liquid interface. Thus for normal incidence, the equal intensities of the circular polarized pump light along all in-plane directions yield in-plane isotropic distributions of both ground and excited molecules. There is therefore no time dependent change in the in-plane orientational distribution because the in-plane distribution of molecules, both excited and ground-state are isotropic in the plane of the interface. Thus the kinetics observed are due only to the out-of-plane motions of the C314 molecules. The circular polarized pump perturbs the equilibrium orientational distribution in the polar angle θ, because absorption is favored by C314 molecules that have their transition dipole moment $\vec{\mu}$ at large values of θ. Therefore, the probability for the excitation of a ground-state molecule whose transition dipole moment is oriented with angle θ is determined by

$$|\vec{\mu} \cdot \vec{E}_{\mathrm{c}}|^2 = \mu^2 E_{\mathrm{c}}^{\,2} \sin^2\theta \qquad (3)$$

where $\vec{E}_{\mathrm{c}}$ is the electric field of the normal incident circularly polarized pump.

Prior to the excitation pulse, the ground-state equilibrium susceptibility element $\chi^{(2)}_{XXZ}(\mathrm{eq})$ can be expressed as

$$\chi^{\mathrm{SF}}_{\mathrm{g},XXZ}(\mathrm{eq}) = N_{\mathrm{g}}(t<0)\int [\alpha^{\mathrm{SF}}_{\mathrm{g},zzz}\ell_{Xz}{}^2\ell_{Zz} + \alpha^{\mathrm{SF}}_{\mathrm{g},xxz}\ell_{Xx}{}^2\ell_{Zz} + \\ \alpha^{\mathrm{SF}}_{\mathrm{g},yyz}\ell_{Xy}{}^2\ell_{Zz}]\rho_{\mathrm{g}}(\Omega_0, t<0)\,\mathrm{d}\Omega_0 \qquad (4)$$

On integrating over the Euler angles, an equation that depends on θ_0 only is obtained.

$$\chi^{\mathrm{SF}}_{\mathrm{g},XXZ}(\mathrm{eq}) = N_{\mathrm{g}}(t<0)\alpha^{\mathrm{SF}}_{g,zzz}\int_0^{\pi} \mathrm{d}\theta_0\, \rho_{\mathrm{g}}(\theta_0, t<0)[\cos\theta_0 - \\ \cos^3\theta_0 + r(\cos^3\theta_0 + \cos\theta_0)] \qquad (5)$$

where $N_{\mathrm{g}}(t < 0)$ is the density of interfacial ground-state molecules prior to pump excitation and $\rho_{\mathrm{g}}(\Omega_0, t < 0)$ is the orientational probability distribution of the ground-state molecules prior to the excitation, ℓ_{Zz}, ℓ_{Xx}, and ℓ_{Yz} are the direction cosines of the molecular axes of the carbonyl group with the laboratory axes, $\alpha^{(2),\mathrm{SF}}_{xxz} = \alpha^{(2),\mathrm{SF}}_{yyz}$ by symmetry, and

$$r = \frac{\alpha^{(2),\mathrm{SF}}_{xxz}}{\alpha^{(2),\mathrm{SF}}_{zzz}} = \frac{\alpha^{\mathrm{Raman}}_{xx}\mu_z}{\alpha^{\mathrm{Raman}}_{zz}\mu_z} = \frac{\alpha^{\mathrm{Raman}}_{xx}}{\alpha^{\mathrm{Raman}}_{zz}} \qquad (6)$$

which is the ratio of the Raman polarizability elements perpendicular (x, y) and parallel (z) to the C=O bond, μ_z is the infrared vibrational transition matrix element, and other constants have been set to unity. After excitation, the total susceptibility is

$$\chi^{(2)}_{\mathrm{Total},XXZ}(t) = \chi^{(2)}_{\mathrm{g},XXZ}(t) + \chi^{(2)}_{\mathrm{e},XXZ}(t) \qquad (7)$$

where the subscript e refers to the ensemble of excited-state C314 molecules and g refers to the ground-state molecules. The time-dependent ground-state contribution arises from those ground-state molecules that were not photoexcited by the pump pulse as they reorient to achieve their equilibrium distribution $\rho_{\mathrm{g}}(\Omega_0, t < 0)$. Similarly the photoexcited molecules reorient to the excited-state equilibrium distribution. It is not necessary to include the contribution of ground-state molecules that were initially photoexcited and then decayed to the ground state because the population recovery time is long compared with rotational times.[17]

The number density of ground-state molecules having an orientation Ω at a time t after the pump pulse is given by $N_{\mathrm{g}}(\Omega, t) = N_{\mathrm{g}}(t)\rho_{\mathrm{g}}(\Omega, t)$, where $\rho_{\mathrm{g}}(\Omega, t)$ is the probability that a ground-state molecule has an orientation Ω at time t. The ground-state susceptibility at time t can be written as

$$\chi^{\mathrm{SF}}_{g,XXZ}(t) = N_{\mathrm{g}}(t)\int_{\Omega} [\alpha^{\mathrm{SF}}_{\mathrm{g},zzz}\ell_{Xz}{}^2\ell_{Zz} + \alpha^{\mathrm{SF}}_{\mathrm{g},xxz}\ell_{Xx}{}^2\ell_{Zz} + \\ \alpha^{\mathrm{SF}}_{\mathrm{g},yyz}\ell_{Xy}{}^2\ell_{Zz}]\rho_{\mathrm{g}}(\Omega, t)\,\mathrm{d}\Omega \qquad (8)$$

On integrating over the Euler angles, an expression that is only a function of θ is obtained,

$$\chi^{\mathrm{SF}}_{\mathrm{g},XXZ}(t) = N_{\mathrm{g}}(t)\alpha^{\mathrm{SF}}_{\mathrm{g},zzz}\int_0^{\pi} \mathrm{d}\theta\, [(\cos\theta - \cos^3\theta) + r(\cos\theta - \\ \cos^3\theta)]\rho_{\mathrm{g}}(\theta, t) \qquad (9)$$

The excited-state susceptibility element $\chi^{(2),\mathrm{SF}}_{\mathrm{e},XXZ}(t)$ at time t is similar to eq 9 where now it is the excited-state population N_{e}, the hyperpolarizability elements e.g. $\alpha^{(2),\mathrm{SF}}_{\mathrm{e},yyz}$ are for the excited-state molecules, and the orientational probability function is for

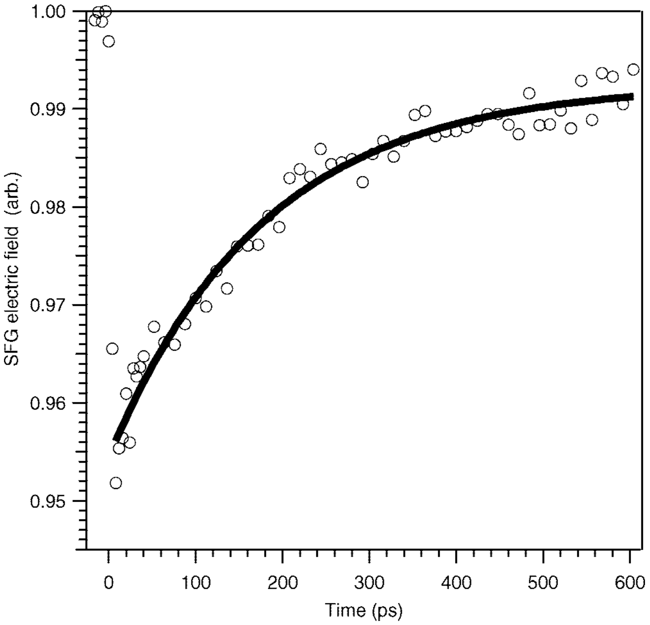

Figure 3. Sum frequency electric field as a function of pump-SFG delay time. Coumarin 314 molecules at the air/water interface were probed by 5.7 μm femtosecond IR light plus the 400 nm picosecond light. C314 was pumped by femtosecond 423 nm circularly polarized light incident along the surface normal. The solid line is a fit to a single exponential giving 220 ± 20 ps. The data for times earlier than 12 ps are not included to eliminate contributions from the solvation dynamics.

the excited-state molecules $\rho_e(\Omega, t)$. The orientational probability functions for the ground state $\rho_g(\Omega, t)$ and excited state $\rho_e(\Omega, t)$ evolve in time as the ground-state and excited-state molecules rotate toward their orientational equilibrium distributions. The evolution of $\rho_g(\Omega, t)$ can be written as[51]

$$\rho_g(\Omega, t) = \int_{\Omega_0} \rho_g(\Omega_0, 0) G(\Omega_0, 0|\Omega, t)\, d\Omega_0 \qquad (10)$$

where $\rho_g(\Omega_0, 0)$ is the probability distribution immediately after the pump photoexcitation at $t = 0$ and the evolution function $G(\Omega_0, 0|\Omega, t)$ describes the rotation of a molecule from an orientation Ω_0 at $t = 0$ to the orientation Ω at time t. For orientational relaxation in bulk liquids, the evolution function can be obtained from solution of the rotational diffusion equation. At the interface, there is no such equation for an adsorbed molecule, which necessarily experiences an anisotropic friction that is furthermore dependent on the location of the molecule in the interfacial region. Simulations offer the best possibility at this time to describe interfacial molecular motions.[52,53] Because the excited-state solvation, the orientational relaxation and the population recovery are well separated in time, their dynamics can be differentiated in pump−probe experiments. For C314 at the air/water interface, the excited-state decay time is 4.5 ns,[17] the out of plane orientational relaxation time is 343 ± 13 ps,[17,18] and the excited-state solvation times are 250 ± 50 fs and 2.0 ± 0.4 ps.[38,54]

In both the SFG and SHG experiments, the same nonequilibrium orientational distribution is induced by the pump pulse. For the purpose of comparison, the ground-state susceptibility element appropriate for SHG experiment is

$$\chi^{\mathrm{SH}}_{g,XXZ}(t) = N_g(t)\alpha^{\mathrm{SH}}_{g,zzz} \int_0^{\pi} d\theta\, (\cos\theta - \cos^3\theta)\rho_g(\theta, t) \qquad (11)$$

As shown in Figure 3, the out of plane orientation relaxation dynamics for the SFG experiments yield a time constant of 220 ± 20 ps that was obtained using a single exponential fit. There was no improvement in the fit using a multiexponential function. The excellent fit to a single exponential function indicates that the rotational dynamics of the ground-state and excited-state molecules are similar. Apparently, the larger dipole moment of the excited-state molecule, which is 4 Debye larger than the ground-state molecules, does not sufficiently reorganize the surrounding water molecules to change the rotational friction to an extent that could be detected with the signal/noise of our experiment. In contrast to the SFG findings, the results obtained from the SHG probe experiments for C314 at the air/water interface were found to be significantly slower, 343 ± 13 ps. The key difference between the SHG and SFG probe experiments is that the rotational motions of different molecular axes are being measured. In the SHG experiments, it is the rotation of the $S_0 \rightarrow S_1$ transition dipole moment axis, which is also the permanent dipole moment axis, which is rotating with respect to the interface normal. On the other hand, it is the reorientational motions of the carbonyl bond axis that is probed in the SFG experiments.

It is not surprising perhaps that the reorientational dynamics differs significantly considering the fact that the susceptibility elements differ and the rotational motions of the transition dipole axis and the carbonyl bond axis, which necessarily have different orientations at the interface, experience different rotational frictions. Although the coumarin 314 molecule is a rigid structure, the rotational motions about different molecular axes, for example, the permanent dipole and the carbonyl axis, can experience different frictions. The rotation about axes that would bring the carbonyl group to orientations closer to the air side of the interface and for which it would not be, or only weakly hydrogen bonded, would be energetically unfavorable. On the other hand, rotations that change the orientation of the permanent dipole without markedly altering the orientation of the carbonyl groups could be energetically more favorable. In other words, the energy profile of rotation about various axes are likely to differ and therefore have different resistances to particular rotations. Although there are no rigorous treatments of interfacial molecular rotation, the diffusion in a cone model provides some qualitative insight to the orientational dynamics.[55,56] In this model the rotational motion of a rod is restricted to rotation in a conical volume. The application of this model to the time-dependent change for both SFG and SHG experiments yields a multiexponential decay of both the SFG and SHG intensities, which we have not observed within our experimental error. However, the model predicts, as is intuitively reasonable, that the rotational diffusion is faster for narrower cones, i.e. a smaller range of the polar angle results in a faster reorientation, provided of course the rotational friction is the same for the larger and smaller cones. It is likely that the carbonyl group in the ring of coumarin 314 is hydrogen-bonded to water so that its orientational distribution is narrower than that of the transition dipole moment axis, which is probed in the SHG measurements. The narrower orientation distribution of the carbonyl group implies that a smaller change in the orientation angle is required to achieve equilibrium. This could result in faster orientational dynamics of the carbonyl bond axis than the transition dipole moment axis, which could be a factor in the faster reorientation obtained in the SFG experiments.

4. Conclusions

The time dependent changes in an ensemble of ground- and excited-state molecules at a liquid interface have been measured for the first time using sum frequency generation (SFG). The evolution of the nonequilibrium orientational distribution of ground and excited molecules induced by a 130 fs pump pulse is monitored by SFG. By selecting the polarization of the pump pulse to be circularly polarized and incident along the normal to the interface, it is possible to measure rotational motions that are only the out-of-plane interfacial motions, i.e. changes in the polar angle of a given molecular axis. The out-of-plane orientational relaxation time for rotation of the —C=O bond axis with respect to the interface normal is found to be 220 ± 20 ps at the air/water interface. The dynamics followed a single exponential decay, which was not improved by a double exponential fit. This finding indicates that the orientational relaxation time of ground-state and excited-state molecules can be considered as equal within the signal/noise of the experiment. The orientational relaxation of the carbonyl group is significantly faster than the rotation of the C314 permanent dipole moment axis, 343 ± 13 ps, as obtained from pump-SHG-probe studies. Possible effects of the hydrogen bonding of the carbonyl group with interfacial water, on the reorientational dynamics, and a rotational diffusion in a cone model, are discussed briefly. By combining the findings of the SFG and SHG experiments the equilibrium absolute orientation of the C314 molecule at the air/water interface is obtained.

Acknowledgment. The authors thank the National Science Foundation, the Chemical Sciences, Geosciences and Biosciences Division, and the Office of Basic Energy Sciences, Office of Science, US Department of Energy, as well as DTRA (W911NF-07-1-0116).

References and Notes

(1) Adamson, A. *Physical Chemistry of Surfaces*, 5th ed.; John Wiley and Sones, Inc.: New York, 1990.

(2) Israelachvili, J. N. *Intermolecular And Surface Forces*, 2nd ed.; Academic Press: London, 1991.

(3) Berkowitz, M. L.; Bostick, D. L.; Pandit, S. *Chem. Rev.* **2006**, *106*, 1527.

(4) Verdaguer, A.; Sacha, G. M.; Bluhm, H.; Salmeron, M. *Chem. Rev.* **2006**, *106*, 1527.

(5) Eisenthal, K. B. *Chem. Rev.* **2006**, *106*, 1462.

(6) Chang, T. M.; Dang, L. X. *Chem. Rev.* **2006**, *106*, 1305.

(7) Benjamin, I. *Chem. Rev.* **2006**, *106*, 1212.

(8) Jungwirth, P.; Finlayson-Pitts, B. J.; Tobias, D. J. *Chem. Rev.* **2006**, *106*, 1137.

(9) Shen, Y. R.; Ostroverkhov, V. *Chem. Rev.* **2006**, *106*, 1140.

(10) Gopalakrishnan, S; Liu, D. F.; Allen, H. C.; Kuo, M.; Shultz, M. J. *Chem. Rev.* **2006**, *106*, 1155.

(11) Shen, Y. R. *Annu. Rev. Phys. Chem.* **1989**, *40*, 327–350.

(12) Eisenthal, K. B. *Chem. Rev.* **1996**, *96*, 1343–1360.

(13) Richmond, G. L. *Chem. Rev.* **2002**, *102*, 2693–2724.

(14) Wang, H. F.; Gan, W.; Lu, R.; Rao, Y.; Wu, B. *Int. Rev. Phys. Chem.* **2005**, *24*, 191–256.

(15) Castro, A.; Sitzmann, E. V.; Zhang, D.; Eisenthal, K. B. *J. Phys. Chem.* **1991**, *95*, 6752–6753.

(16) Wirth, M. J.; Burbage, J. D. *J. Phys. Chem.* **1992**, *96*, 9022.

(17) Zimdars, D.; Dadap, J. I.; Eisenthal, K. B.; Heinz, T. F. *J. Phys. Chem. B* **1999**, *103*, 3425–3433.

(18) K. T., Nguyen; Shang, X. M.; Eisenthal, K. B. *J. Phys. Chem. B* **2006**, *110*, 19788–19792.

(19) Shultz, M. J.; Schnitzer, C.; Baldelli, S. *Int. Rev. Phys. Chem.* **2000**, *19*, 123–153.

(20) Corn, R. M.; Higgins, D. A. *Chem. Rev.* **1994**, *94*, 107–125.

(21) Simpson, G. J.; Rowlen, K. L. *Anal. Chem.* **2000**, *72*, 3407–3411.

(22) Rao, Y.; Tao, Y. S.; Wang, H. F. *J. Chem. Phys.* **2003**, *119*, 5226–5236.

(23) Petersen, P.; Saykally, R. *J. Phys. Chem. B* **2006**, *110*, 14060.

(24) Wang, H. F.; Troxler, T.; Yeh, A. G.; Dai, H. L. *J. Phys. Chem. C* **2007**, *111*, 8708.

(25) Lu, R.; Gan, W.; Wu, B. H.; Chen, H.; Wang, H. F. *J. Phys. Chem. B* **2004**, *108*, 7297–7306.

(26) Wang, J.; Paszti, Z.; Even, M. A.; Chen, Z. *J. Am. Chem. Soc.* **2002**, *124*, 7016–7023.

(27) Chen, X. Y.; Clarke, M. L.; Wang, J.; Chen, Z. *Int. J. Mod. Phys. B* **2005**, *19*, 691–713.

(28) Levering, L. M; Sierra-Hernandez, M. R.; Allen, H. C. *J. Phys. Chem. C* **2007**, *111*, 8814.

(29) Ma, G.; Allen, H. C. *J. Phys. Chem. B* **2003**, *107*, 6343–6349.

(30) Voges, A. B.; Al-abadleh, H. A.; Musorrariti, M. J.; Bertin, P. A.; Nguyen, S. T.; Geiger, F. M. *J. Phys. Chem. B* **2004**, *108*, 18675–18682.

(31) Esenturk, O.; Walker, R. *J. Chem. Phys.* **2006**, *125*, 174701.

(32) Bordenyuk, A.; Benderskii, A. *J. Chem. Phys.* **2005**, *122*, 134713.

(33) Liu, J.; Conboy, J. *J. Phys Chem C* **2007**, *111*, 8988–8999.

(34) Kataoka, S.; Cremer, P. *J. Am. Chem. Soc.* **2006**, *128*, 5516–5522.

(35) Fourkas, J. T.; Walker, R. A.; Can, S. Z.; Gershgoren, E. *J. Phys. Chem. C* **2007**, *111*, 8902–8915.

(36) Viswanath, P.; Motschmann, H. *J. Phys. Chem. C* **2007**, *111*, 4484.

(37) Sitzmann, E. V.; Eisenthal, K. B. *J. Phys. Chem.* **1988**, *92*, 4579–4580.

(38) Zimdars, D.; Dadap, J. I.; Eisenthal, K. B.; Heinz, T. F. *Chem. Phys. Lett.* **1999**, *301*, 112–120.

(39) Meech, S. R.; Yoshihara, K. *Chem. Phys. Lett.* **1990**, *174*, 423–427.

(40) McArthur, E. A.; Eisenthal, K. B. *J. Am. Chem. Soc.* **2006**, *128*, 1068–1069.

(41) Harris, A. L.; Rothberg, L. *J. Chem. Phys.* **1991**, *94*, 2449–2457.

(42) McGuire, J. A.; Shen, Y. R. *Science* **2006**, *313*, 1945–1948.

(43) Smits, M.; Ghosh, A.; Sterrer, M.; Muller, M.; Bonn, M. *Phys. Rev. Lett.* **2007**, *98*, 098302.

(44) Richter, L. T.; Petralli-mallow, T. P.; Stephenson, J. C. *Opt. Lett.* **1998**, *23*, 1594–1596.

(45) E. L. Hommel, G. M.; H. C. Allen, A. S. *Anal. Sci.* **2001**, *17*, 1–5.

(46) Rao, Y.; Comstock, M.; Eisenthal, K. B. *J. Phys. Chem. B* **2006**, *110*, 17271732..

(47) Raoult, F.; Boscheron, A. C. L.; Husson, D.; Sauteret, C.; Modena, A.; Malka, V.; Dorchies, F.; Migus, A. *Opt. Lett.* **1998**, *23*, 1117–1119.

(48) Zhuang, X.; Miranda, P. B.; Kim, D.; Shen, Y. R. *Phys. Rev. B* **1999**, *59*, 12632–12640.

(49) Wei, X.; Hong, S. C.; Zhuang, X. W.; Goto, T.; Shen, Y. R. *Phys. Rev. E* **2000**, *62*, 5160–5172.

(50) Lu, R.; Gan, W.; Wang, H. F. *Chin. Sci. Bull.* **2003**, *48*, 2183–2187.

(51) Chuang, T. J.; Eisentha, K. B. *J. Chem. Phys.* **1972**, *57*, 5094.

(52) Pantano, D.; Laria, D. *J. Phys. Chem. B* **2003**, *107*, 2971–2977.

(53) Benjamin, I. *J. Chem. Phys.* **2007**, *127*, 204712.

(54) Benderskii, A. V.; Eisenthal, K. B. *J. Phys. Chem. A* **2002**, *106*, 7482–7490.

(55) Wang, C.C.; Pecora, R. *J. Chem. Phys.* **1980**, *72*, 5333–5340.

(56) Tao, T. *Biopolymers* **1969**, *8*, 609–632.

JP802499W